Transformation and Mechanical Behaviour of a Ni47Ti44Nb9 Shape Memory Alloy

Zhao, Duerig, Wayman

Proceedings of the MRS Int'l Meeting on Advanced Materials
"Shape Memory Materials" Vol. 9
pp. 171-176

1989

TRANSFORMATION AND MECHANICAL BEHAVIOR OF A $Ni_{47}Ti_{44}Nb_9$ SHAPE MEMORY ALLOY

L.C.ZHAO, T.W.DUERIG AND C.M.WAYMAN
Harbin Institute of Technology, Harbin, China;
Raychem Corporation, Menlo Park, CA.USA;
University of Illinois, 1304 W. Green St., Urbana, IL.61801, USA.

INTRODUCTION

It has recently been shown [1,2] that NiTiNb shape memory alloys exhibit a wide transformation hysteresis compared to NiTi binary alloys (about 125°C versus 30°C). The hysteresis increases principally because of an increase in the A_s-A_f temperature regime. By "overdeforming" NiTiNb alloys in the martensitic phase (resulting in some irrecoverable strain), the A_s temperature is temporarily increased to A_s', thus permitting couplings and fasteners, to be stored at ambient temperatures. This wide hysteresis has important practical utility for the shape memory field.

For years the transformation and mechanical behavior of nearly stoichiometric TiNi alloys has received extensive attention because of their "premartensitic" phenomena and shape memory effects. Substantial progress has recently been made in understanding of both mechanistic details and mechanical aspects of the transformations in TiNi shape memory alloys [3]. However, all existing reference deals scantly with the phase transformation in NiTiNb [4,5]. The present work was undertaken to investigate the transformation and mechanical behavior of a wide hysteresis $Ni_{47}Ti_{44}Nb_9$ alloy and to discuss the role of Nb additions to this alloys.

EXPERIMENTAL

The alloy composition used for the present study was 47 at% Ni, 44 at% Ti and 9 at% Nb. The test material was supplied by Raychem Corporation with the strips of approximately 0.50mm thickness. The various samples were cut from the strips using a diamond saw and then annealed at 850°C for 30 min in a $5x10^{-5}$ torr vacuum and furnance cooled. The transformation temperatures after this heat treatment were measured by electrical resistance method; M_s, M_f, A_s, A_f temperature were -90, -175, -85 and -35°C, respectively. The final dimensions of the strips samples for electrical resistance measurement were approximately 40 mm in length, 1.0 mm in width and 0.4 mm in thickness.

SEM samples were prepared by mechanical polishing and left unetched. The SEM experiment was carried out in a JSM35C microscope. The precipitate powder for X-ray diffraction study (Deby-Scherrer method) was prepared by electrolytic extraction in 25vol% HNO_3 and 75vol% methanol. The powder photographs were taken with CuK_α radiation (nickel filter).

The TEM foils were prepared by mechanical thinning the 25x8x0.5 mm samples to approximately 100 microns on 180-600 grit SiC paper then punching 3 mm discs and electropolishing in a 15 vol% sulfuric acid-85 vol% methanol mixture at -25°C. The TEM/EDX analysis were carried out in a philips EM 400 operating at 120 KV equipped with energy dispersive X-ray analysis system. The quantitative X-ray analysis using the ratio technique and thin film criterion was performed for the EDX spectra in TEM. Electron diffraction and microscopy were carried out in a Hitachi H-800 microscope operated at 200 KV and equipped with a ±45°, double-tilt stage. An in-situ cooling experiment was performed using a H5001C ±45° tilting-cooling stage which permitted the specimen to be cooled from room temperature to about -120°C.

MRS Int'l. Mtg. on Adv. Mats. Vol. 9 ©1989 Materials Research Society.

A tensile sample was deformed to 16.0% elongation with a deformation rate of $5.29 \times 10^{-4} s^{-1}$ at -60°C. Upon unloading, the strain at room temperature is 10.2%. The TEM foils of the tensile sample were prepared from the gage section of deformed sample.

RESULTS AND DISCUSSION

3.1 Identification of the Niobium-rich Phase

The microstructure is remarkably different from the NiTi binary alloy. After annealing at 850°C for 30 min, an insoluble dispersed phase which exhibits globular or elliptical morphology appears in the matrix, as shown in Figure 1. The coarse blocky dark phase in Figure 1 was shown by SEM/EDX analysis to be a compound of approximate composition $Ti_3 (Ni,Nb)_2$. The present experiments have demonstrated that the above dispersed phase is still insoluble when the specimen was heated to 1100°C. As heating time was extended, the particles of the insoluble phase were grown. Consequently they are precipitates formed at higher temperature; probably during solidification. The chemical composition of both the precipitate and the matrix was examined by TEM/EDX analysis. Figure 2(a) is a TEM micrograph of a same specimen shown in Figure 1, Figure 2(b) and (c) show corresponding EDX spectra taken from a precipitate labeled P in Figure 2(a) and matrix labeled M in Figure 2(a), respectively . In order to avoid the overlapping absorption from the matrix, all EDX spectra of the precipitate were taken from the edge of the hole in thin foil as shown in Figure 2(a). The quantitative compositions of three different points for the precipitates and matrix are presented in Table 1. From this table the matrix is identified as a TiNi phase containing some amount of niobium, while the precipitate is a niobium-rich phase. TEM observation shows that the precipitates are highly dislocated. The results of the X-ray powder diffraction for the precipitate is listed in Table 2. It indicates that both the structure and lattice parameter of the precipitate lie close to the β phase of a NbTi alloy containing 80 at% Nb, which has a body-centered-cubic structure with a lattice parameter of 0.3297nm [6]. The lattice parameter of the niobium-rich precipitate was determined by X-ray to be 0.32963nm. It is thus concluded that the niobium-rich precipitates are body-centered-cubic β-Nb containing some amount of Ni and Ti.

Table 1: TEM/EDX Analysis of Three Different Points for the Precipitate and Matrix in Figure 1(a)

	Ni (at%)	Ti (at%)	Nb (at%)
Precipitate	7.685	11.592	80.723
	6.693	11.637	81.667
	6.359	11.949	81.691
Matrix	48.254	46.008	5.738
	47.094	47.878	5.028
	49.194	44.833	5.973

Table 2: Spacings of the Niobium-rich Precipitate from X-ray Diffraction

Line	Spacing d (nm)	hkl	Observed relative intensity
1	0.22773	110	vs
2	0.16435	200	ms
3	0.13449	211	s
4	0.11646	220	m
5	0.10409	310	ms
6	0.09508	222	mw
7	0.08805	321	ms
8	0.08242	400	w
9	0.07769	411,330	ms

Order of intensities vs>s>ms>mw>w.

3.2 The structure of parent phase

The parent phase was examined by electron imaging and diffraction at room temperature. Figure 3 shows a TEM micrograph and corresponding diffraction pattern series. The mottling "tweed-like" structure as reported earlier in TiNi alloys [7] is observed in Figure 3(a) in addition

Figure 1: Microstructure of $Ni_{47}Ti_{44}Nb_9$ alloy annealed at 850°C for 30 min, composition image (SEM)

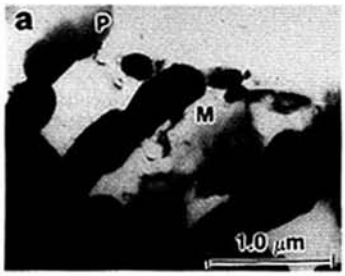

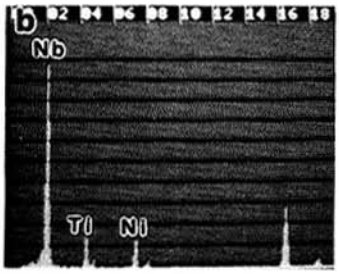

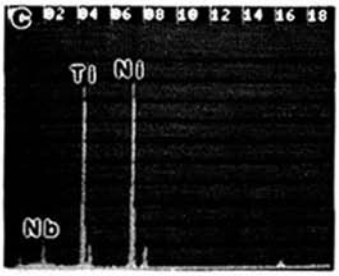

Figure 2: (a) Transmission electrin micrograph of $Ni_{47}Ti_{44}Nb_9$ alloy annealed at 850°C for 30 min, (b) (c) corresponding EDX spectra taken from precipitate labeled P in (a) and matrix labeled M in (a), respectively

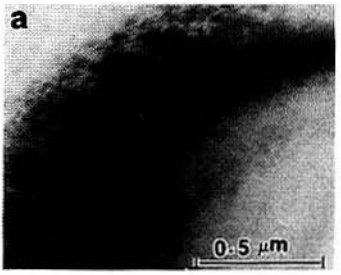

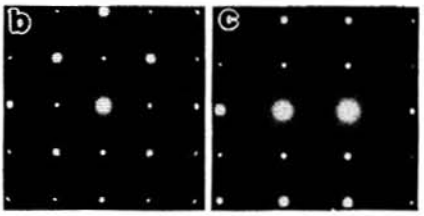

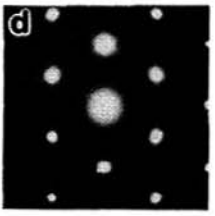

Figure 3: Transmission electron micrograph and corresponding electron diffraction pattern series of the parent phase in $Ni_{47}Ti_{44}Nb_9$ (a) Electron micrograph, (b) $[001]_{B2}$, (c) $[011]_{B2}$, (d) $[111]_{B2}$ the diffuse electron scattering is evident

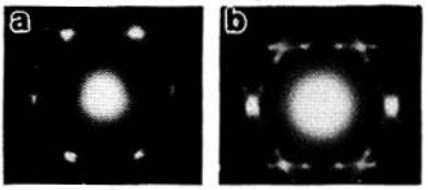

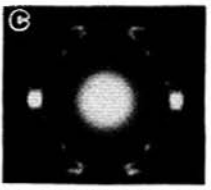

Figure 5: Temperature dependence of 1/3 (110) Superlattice reflection in $[111]_{B2}$ zone, (a) 0°C, (b) -21°C, (c) -38°C

to the usual bending contours. Figures 3(b) to (d) are Selected Area Diffraction (SAD) which are identified as [001], [110], and [111] zones of the CsC1(B2) cubic structure [8]. The lattice parameter of the B2 parent phase was determined by X-ray diffraction to be 0.30182nm. Diffuse scattering can be observed in Figure 3(b) to (d). It shows that the incommensurate phase exist in parent at room temperature.

3.3 The transformation of Parent Phase during Cooling to Lower Temperature

The present experiments show that the parent phase of $Ni_{47}Ti_{44}Nb_9$ alloy exhibits transformation behavior similar to that of nearly stoichiometric NiTi alloys during cooling to lower temperatures. Figure 4 shows an electrical resistivity versus temperature plot between 100°C and liquid nitrogen temperature for the as-annealed sample. Upon cooling, the resistivity starts to increase at T_p, which corresponds to the onset of the incommensurate transformation. At M_s the resistivity starts to decrease continuously until liquid nitrogen temperature. As the specimen was cooled from room temperature, the parent-incommensurate transition occurs. Figure 5 is a sample indicating the temperature dependence of the 1/3(110) super lattice reflection in the [111]B2 zone. The superlattice reflection intensity was increased with decreasing temperature. When the specimen temperature was nearing M_s, needle-like plates were observed (as shown in Figure 6). However, they are confirmed not to be the R-phase by electron and X-ray diffraction and differential scanning calorimetry [9]. As the specimen was cooled below M_s, the martensite plates with regular twin lamellar were seen to grow abruptly to a lenticular shape. In addition to transformational twins, stacking faults were also observed in some martensites. Figure 7(a) and (b) show the martensite with regular twin lamellar and a corresponding SAD pattern derived from the middle area of Figure 7(a). From Figure 7(a) and (b), it is seen that the streaks in Figure 7(b) are perpendicular to the striations in Figure 7(a). These streaks are characteristic of a high density of thin twins. Utilizing dark field techniques, the alternating platelets in Figure 7(a) have been confirmed to be twin related. From Figure 7(a) it is also obvious that APD's (Antiphase Microdomains) are observed in the twin variants of the martensite. Figure 7 (c) and (d) show the stacking faults of the martensite in the $Ni_{47}Ti_{44}Nb_9$ alloy and a corresponding SAD pattern derived from the middle area Figure 7(c). The striations in Figure 7(c) are perpendicular to the long diffuse streaks along the [001] reciprocal lattice direction of the diffraction pattern in Figure 7(d). Consequently the striations in Figure 7(c) are parallel to the (001) plane, which is the basal plane of the martensite. This implies the stacking faults to be on the (001) basal plane.

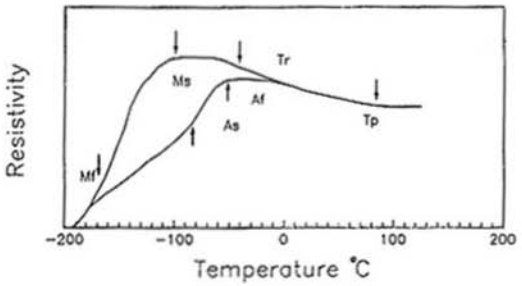

Figure 4: Electrical resistivity vs. temperature plot of $Ni_{47}Ti_{44}Nb_9$ alloy for a full thermal cycle between 100°C and liquid nitrogen temperature

3.4 Deformation Behavior Associated with Martensite Transformation and Niobium-rich Precipitates

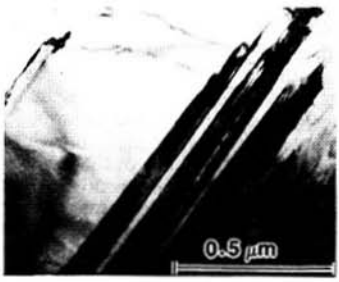

Figure 6: Needle-like Plates in $Ni_{47}Ti_{44}Nb_9$ alloy at -80°C

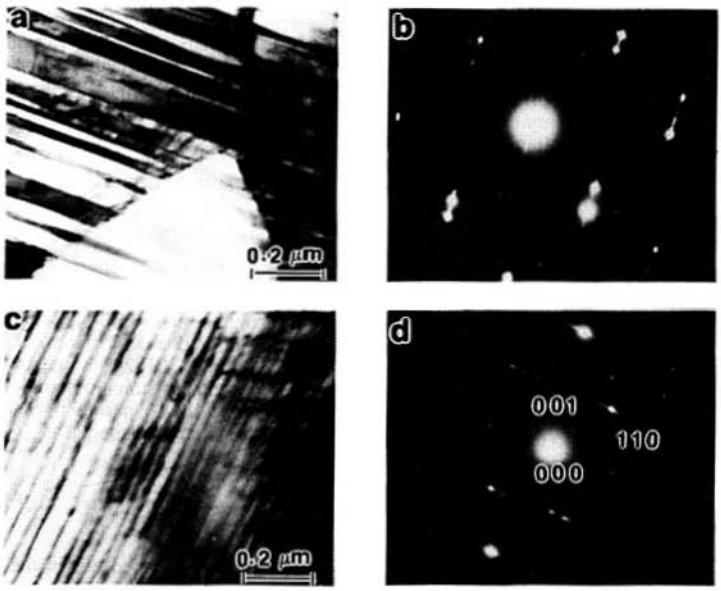

Figure 7: Internal defects of martensites in $Ni_{47}Ti_{44}Nb_9$ alloy at -105°C,.(a) Bright field image of twin martensite (b) Corresponding electron diffraction pattern (c) Bright field image of martensite showing stacking faults (d) Corresponding diffraction pattern

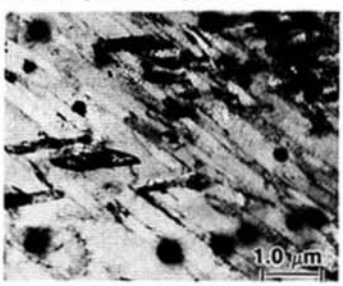

Figure 8: Bright field image of microstructure at room temperature for annealed $Ni_{47}Ti_{44}Nb_9$ specimen deformed to 16% at -60°C.

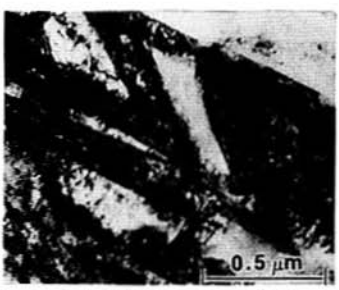

Figure 9: Bright field image show self-accommodation of strain martensites.

The present experiment shows that the width of the transformational hysteresis for undeformed $Ni_{47}Ti_{44}Nb_9$ specimens annealed at 850°C is about 55°C (M_s=-90°C, A_s=-35°C). This hysteresis width can be increased to 150°C with a 16% tensile deformation at -60°C. In this case, M_s will stay at about -90°C, while A_s is raised to 60°C. It is obvious that the transformational hysteresis after deforming at -60°C is remarkably increased. Figure 8 shows the microstructure at room temperature for the same tensile specimen. The fine deformed martensite exists between the niobium-rich precipitates. Figure 9 also shows that niobium-rich precipitates prevent matrix recrystallization so that the extremely fine dimensions of the matrix grains are evident. In general, the average grain diameter is about 1.5 μm. Consequently the formation of fine martensites is due to the refinement of matrix grains and the partitioning effect of the niobium-rich precipitates dispersed in matrix. Figure 9 shows that the stress induced martensite in the strained specimen exhibits a self-accommodation morphology. It can be seen from Figure 8 that the martensite plates in the deformed condition are often near β-Nb precipitates. We speculate that the β-Nb precipitates probably decrease the elastic strain energy of the martensite near the β-Nb precipitates: In this case, the existence of β-Nb precipitates leads to the stabilization of strain martensite. The present experiment found that the strained martensite has an irregular twin substructure probably including some dislocations. To summarize the microstructure of the $Ni_{47}Ti_{44}Nb_9$ shape memory alloy is a hard ordered matrix (TiNi phase) containing fine dispersion of a soft second phase (β-Nb). The transformation characteristics of this alloy is that the soft precipitates dispersed in matrix give rise to a refinement of the strain martensite formed by deformation, and more often than not leading to the formation of strain martensite near soft precipitates. This decreases the elastic strain energy of the martensite resulting in a lower driving force for the reverse transformation. Consequently, the A_s temperature of this alloy can be raised by deformation.

CONCLUSIONS

Nb additions to NiTi lead to the formation of an insoluble phase of β-Nb which exhibit a globular or elliptical morphology. The phase is cubic (disordered a=0.32963nm) and is highly dislocated. The parent phase is an ordered Cubic TiNi phase (a=0.30182nm) containing about 5 at % niobium and exhibits transformation behavior similar to that of stoichiometric TiNi alloys. Upon cooling the sequence of transformation event is as follows: parent phase B2 to the incommensurate phase to needle-like plates (not yet identified) to martensite phase. The effect of the soft β-Nb particles is to increase transformational hysteresis.

ACKNOWLEDGMENTS

The SEM/EDX and TEM/EDX analysis of this work was carried out in the center for microanalysis of materials University of Illinois which is supported by the U.S. Department of Energy under contract De-Ac 02-76 ER01198. The authors are grateful to senior microprobe analyst J. B.Woodhouse and research metallurgist P.Mochel for the cooperation in the part work.

REFERENCES

1. K.N.Melton, J.Simpson and T.W.Duerig, Proc. Int.Conf. Martensite, Jap. Inst. Met., 1053 (1986).
2. K.N.Melton, J.L.Proft and T.W.Duerig, "Wide Hysteresis Shape Memory Alloys Based on the Ni-Ti-Nb System", Inst. MRS meeting (1988).
3. C.M.Wayman, Plenary Lecture for Presentation at Phase Transformations '87, July 6-10, University of Cambridge, England.
4. Kiyoshi Kamiti, et al., 1987 Autumn Meeting in Japan, October 9-11 (1987).
5. M.I.Zakharova and A..Khundzhua, Izv. Akad. Nauk SSSR Phy., 44, 2193 (1980).
6. Bulletin of Alloy Phase Diagrams, Vol.2, No.1, 55 (1981).
7. C.M.Hwang and C.M.Wayman, Acta Metall., 32, 183 (1984).
8. P.B.Hirsch, et al., Electron Microscopy of Thin Crystals, Robert E. Krieger Publishing Co., New York, NY, P.56 (1977).
9. L.C.Zhao, et al., Work conducted at Raychem in 1988, to be published.